AD-A183 250 IMPEDANCE AND ADMITTANCE MEASUREMENTS AT INTERCALATED 1/1
N-HFS2/NON-AQUEOUS ELECTROLYTE INTERFACE(U) ELTRON
RESEARCH INC AURORA IL K W SEMKOW ET AL. JUL 87 TR-3
UNCLASSIFIED N00014-86-C-0128 F/G 7/2 NL

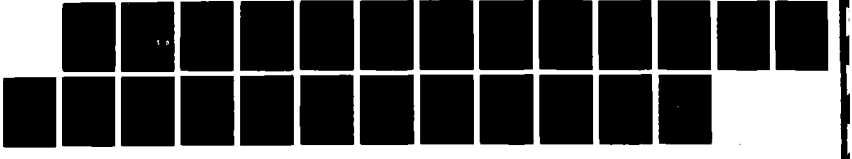

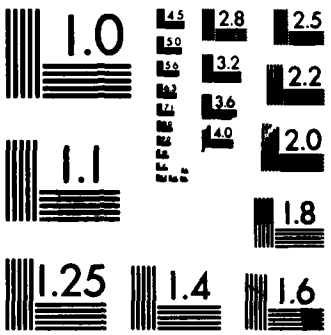

(12)

SECURITY CLASSIFICATION OF THIS PAGE (When Data Entered)

REPORT DOCUMENTATION PAGE

READ INSTRUCTIONS BEFORE COMPLETING FORM

REPORT NUMBER: 3	2. GOVT ACCESSION NO.
3. RECIPIENT'S CATALOG NUMBER	
4. TITLE (and Subtitle): Impedance and Admittance Measurements at Intercalated n-HfS_2/Non-Aqueous Electrolyte Interface	5. TYPE OF REPORT & PERIOD COVERED: Technical, Oct. 1986 - July 1987
6. PERFORMING ORG. REPORT NUMBER	
7. AUTHOR(s): K. W. Semkow, N. U. Pujare and A. F. Sammells	8. CONTRACT OR GRANT NUMBER(s): N00014-86-C-0128
9. PERFORMING ORGANIZATION NAME AND ADDRESS: Eltron Research, Inc., 4260 Westbrook Drive, Aurora, IL 60504	10. PROGRAM ELEMENT, PROJECT, TASK AREA & WORK UNIT NUMBERS
11. CONTROLLING OFFICE NAME AND ADDRESS: Office of Naval Research/Chemistry Program, Arlington, VA 22217	12. REPORT DATE: July 1987 13. NUMBER OF PAGES: 22
14. MONITORING AGENCY NAME & ADDRESS (if different from Controlling Office): Above	15. SECURITY CLASS. (of this report): Unclassified 15a. DECLASSIFICATION/DOWNGRADING SCHEDULE

16. DISTRIBUTION STATEMENT (of this Report)

Approved for public release, distribution unlimited.

17. DISTRIBUTION STATEMENT (of the abstract entered in Block 20, if different from Report)

Approved for public release, distribution unlimited.

18. SUPPLEMENTARY NOTES

Submitted: Journal of the Electrochemistry Society

19. KEY WORDS (Continue on reverse side if necessary and identify by block number)

Hafnium disulfide, capacitance, impedance, admittance spectroscopy, copper intercalation.

20. ABSTRACT (Continue on reverse side if necessary and identify by block number)

Capacitance, impedance and admittance studies were performed on single crystal n-HfS_2 before and after copper intercalation from acetonitrile based electrolyte. The n-HfS_2/non-aqueous electrolyte interface was modelled by equivalent R-C circuits containing frequency dependent elements. Electrochemical intercalation by copper into n-HfS_2 introduced Faradaic conductance effects. The composition of copper intercalated n-HfS_2 in close proximity to the interfacial region was obtained assuming a diffusion coefficient for copper in n-HfS_2 of $\sim 10^{-8} cm^2/sec$. The photoanode demonstrated apparent degeneracy for > 0.1 moles of intercalated copper,

DD FORM 1473 (JAN 73) EDITION OF 1 NOV 65 IS OBSOLETE

Unclassified

SECURITY CLASSIFICATION OF THIS PAGE (When Data Entered)

IMPEDANCE AND ADMITTANCE MEASUREMENTS AT INTERCALATED n-HfS_2/NON-AQUEOUS ELECTROLYTE INTERFACE

Krystyna W. Semkow*, Nirupama U. Pujare and Anthony F. Sammells*

Eltron Research, Inc.
Aurora, Illinois 60504

ABSTRACT

Capacitance, impedance and admittance studies were performed on single crystal n-HfS_2 before and after copper intercalation from acetonitrile based electrolyte. The n-HfS_2/non-aqueous electrolyte interface was modelled by equivalent R-C circuits containing frequency dependent elements. Electrochemical intercalation by copper into n-HfS_2 introduced Faradaic conductance effects. The composition of copper intercalated n-HfS_2 in close proximity to the interfacial region was obtained assuming a diffusion coefficient for copper in n-HfS_2 of $10^{-8}cm^2/sec$. The photoanode demonstrated apparent degeneracy for > 0.1 moles of intercalated copper, suggesting that progressive electronic population of the n-HfS_2 conduction band was occurring. Capacitance values for intercalated n-HfS_2 were of the order $10^{-6}F/cm^2$.

*Electrochemical Society Active Member

Key words: hafnium disulfide, copper intercalation, impedance, capacitance, admittance measurements

Group IVB transition metal dichalcogenides (TMDs) comprising HfS_2, $HfSe_2$, ZrS_2 and $ZrSe_2$ are interesting materials for photoelectrochemical (PEC) study since they can in principle function as both a photoelectrode and simultaneously as the substrate electroactive material for the reversible intercalation of transition metal species[1-13]. For example, it has already been reported that ZrS_2 and HfS_2 are capable of maintaining their semiconducting properties after partial electrochemical intercalation by either Cu or Fe to form ZrM_yS_2 and HfM_yS_2 over the compositional range $0 < y < 0.22$[13]. Such intercalation does however result in a decrease of the band gap width. The group IVB TMDs have also been shown susceptible to cathodic intercalation by alkali and alkaline earth metals and organic species[7-12]. As expected, intercalation into these materials results in a widening of the van der Waals layers[14]. Group IVB TMDs possess an octahedral structure with electron photoexcitation within the semiconductor band gap proceeding from energy bands derived from bonding sulfur p-orbitals into metal t_{2g} d-orbitals[6]. These photoelectrodes possess indirect band gaps with high absorption coefficients, since most incident photons become captured within 1000Å from the interfacial region[15].

Insight gained relating the dependency of photoelectrode properties for these materials on the presence or absence of intercalated metal species, will be of value for identifying conditions where they might be incorporated into PEC cells possessing in situ electrochemical energy storage. Work reported here applies impedance and admittance measurement techniques to single crystal n-HfS_2 materials in non-aqueous electrolyte, oriented parallel to the c-lattice vector (⊥-c) where a high population of intercalation sites would be exposed. Measurements were performed on this photoanode before and after electrochemical intercalation by copper which allowed us to preliminarily model the interfacial region. From such information liquid non-aqueous electrolyte and solid polymer electrolyte PEC storage cells using this photoanode might be more systematically prepared.

EXPERIMENTAL

Single crystals of n-HfS_2 were prepared by the halogen (I_2) vapor transport technique (Northwestern University). Initial solid-state chemical reaction between Hf (99.5%) and S (99.999%) was accomplished by heating an intimate mixture together with 5mg I_2/ml of the quartz transport tube volume. This was performed in a three temperature zone furnace. Typical thermal gradients used

were between 875°C and 800°C. Crystal growth occurred over 25 days. In all cases the relatively large crystals obtained were intrinsically n-type. Ohmic contact to n-HfS_2 was accomplished by sparking indium onto one side of the crystal using a 15 volt DC power supply. This was performed using a fine indium wire as a cathode with the other pole of the power supply clamped to the n-HfS_2 single crystal. When the indium wire was within ≈1mm of the crystal, a transient spark could be observed. This resulted in ion implantation of indium into the ohmic contact region. Current collection was performed with a nichrome wire attached with silver epoxy and cured at 120°C for 1h. Photoelectrodes were then appropriately isolated from later contact with the electrolyte by epoxy (Norton Chemplast), so that only the single crystal front face of interest was exposed. Typical photoelectrode areas for ⊥-c oriented crystals were 0.06cm^2.

Measurements were performed in a standard glass H-cell arrangement using a platinum counter electrode. SCE was used as a reference to the working electrode compartment via a salt bridge. Photoelectrode potentials were controlled by a Stonehart Associates BC 1200 potentiostat. Impedance, conductance and capacitance measurements were performed using a Hewlett-Packard 4276A digital LCZ meter over the frequency range 20kHz-100Hz.

RESULTS AND DISCUSSION

Work performed was directed towards investigating the interfacial characteristics of single crystal n-HfS_2 in liquid non-aqueous electrolyte (acetonitrile containing 0.1M tetrabutylammonium hexafluorophosphate ($TBAPF_6$) as the supporting electrolyte) in the presence of 0.001M CuCl, both with and without copper intercalation. From capacitance, impedance and admittance measurements the n-HfS_2/liquid junction could be modelled by an equivalent circuit which incorporated frequency dependent resistances, R_v, capacitances, C_v, together with the n-HfS_2 space charge capacitance, C_{sc} and the cell resistance R_{el}. The presence of frequency dependent elements may originate from a variety of charge accumulation modes such as surface states caused by adsorption, inhomogeneous doping and crystal defects. Expressions for the total admittance Y, impedance Z, conductance G, and susceptance B, for an equivalent circuit consisting of a large number of R-C elements, could be represented by the following relationships[16,17]:

$$Y = a\omega^n + kb\omega^n \quad (1)$$

$$Z = A\omega^{-n} - jB\omega^{-n} \quad (2)$$

$$G = a\omega^n \quad (3)$$

$$B = b\omega^n \quad (4)$$

where A, B, a, b and n are characteristic circuit constants and ω is the angular frequency.

Impedance and admittance responses for ||-c oriented n-HfS_2/acetonitrile interface were performed over the frequency range 20kHz to 100Hz in the dark. The impedance and admittance results for this interfacial region in the absence of any copper intercalation within the n-HfS_2 or copper present in the electrolyte are shown respectively in Figures 1 and 2. The dark photoelectrode possessed an initial open-circuit potential (OCP) of -0.295V vs. SCE. The impedance data (Figure 1) could be approximated by two linear regions corresponding to high and low frequencies. From our previously reported work[18] on -c oriented n-HfS_2, linear dependencies were found between real and imaginary impedance over this whole frequency range for dark photoelectrode possessing an OCP of -0.103V, however at -0.253V two linear regions were observed, analogous to the result obtained here. A change in dependence between real and imaginary parts of the cell impedance with frequency, as in Figure 1, suggested a complex equivalent circuit for the interfacial region in which the impedance response of one part predominates at low and another part at higher frequencies. From this data the cell resistance (R_{el}) was obtained by extrapolating the high frequency impedance data to infinite frequency giving $R_{el} = 165\Omega$.

The admittance data shown in Figure 2 gave a semicircular plot possessing a radius of 6×10^{-3} $1/\Omega$, equivalent to $1/R_{el}$. No additional semicircular regions were observed indicating a different frequency dependence of admittance at high and low frequencies. Therefore, if the n-HfS_2 interfacial region could be represented by one general equivalent circuit acting as two separate circuits responsive to respectively high and low frequency regions, their time constants must be similar[19,20]. Impedance and admittance responses for the ||-c oriented n-HfS_2 interface can be explained by the equivalent circuits shown in Figure 3a. In this figure C_{sc} represents a frequency independent capacitance attributed to the photoanode space charge capacitance while C_v and R_v represent the frequency dependent capacitance and resistance, respectively, operating in high

and low frequency regions. The magnitude of C_{sc} is usually relatively small compared to C_v and in the low frequency region its contribution can be neglected[19,20]. The network operating at higher frequencies (A) accounts for the linear impedance response observed above 1kHz, crossing the real impedance axis at R_{el} (Figure 1) as well as for a semicircular admittance response of radius $1/R_{el}$ (Figure 2). Another network (B) accounts for a change in impedance slope at frequencies below 1kHz and appears to possess a semicircular response analogous to that found at high frequencies. Upon introducing 0.001M CuCl into the above cell, the dark n-HfS_2 OCP changed from -0.295V to -0.11V vs. SCE. Copper intercalation proceeded into the n-HfS_2 by potentiostatting the electrode at -0.26V vs. SCE when a steady-state cathodic current of the order of ≈10μA occurred. The cathodic electrochemical intercalation of n-HfS_2 by copper could proceed in the dark since the necessary electrons are present as majority carriers. Impedance and admittance data were obtained after respectively 42 min. and 129 min. after initiating intercalation (Figures 4 and 5). Assuming a diffusion coefficient for copper intercalation of $D = 10^{-8}cm^2/sec$, then a mean intercalation depth X given by equation (5) can be calculated:

$$X = \sqrt{2Dt} \qquad (5)$$

and the respective degree of intercalation to this depth X after 42 and 129 min. would correspond to the stoichiometries $HfCu_{0.18}S_2$ and $HfCu_{0.3}S_2$. The impedance data obtained (Figures 4 and 6) approximated a linear relationship between real and imaginary parts in the low frequency region with a circular dependence being observed at higher frequencies. This latter observation suggested an additional resistive element in parallel to the variable resistance in the network operating in the high frequency region shown in Figure 3a. A value for this new resistance R_o was estimated on the basis of the semicircular radius drawn through experimental data in this high frequency region. For n-HfS_2 copper intercalated for 42 min. R_o was found to be of the order ≈200Ω. Such resistance was not found in the absence of copper intercalation suggesting that R_o may represent resistance for reversible intercalation by copper in n-HfS_2.

At measurement frequencies below 1kHz the imaginary part of the cell impedance was found to decrease by an order of magnitude after initial copper intercalation and progressively decreased upon further intercalation as shown by reference to Figures 1, 4 and 6. This observation suggested an increased capacitive cell response in the low frequency region attributable to the presence of intercalated

copper. Similar conclusions could also be drawn from the admittance data shown in Figures 2, 5 and 7. For measurement frequencies below ≈1kHz copper intercalated n-HfS_2 showed higher susceptance values (Figures 5, 7) compared to when copper was absent (Figure 2). This suggests the presence of a capacitive element associated with Faradaic copper intercalation C_o, in series with R_o in this lower frequency range.

Admittance data obtained after respectively 42 and 129 min. of copper intercalation demonstrated a semicircular response in both the low and high frequency region as shown respectively in Figure 5 and 7. This observation may be attributable to differences in time constants for predominant circuit elements operating in high and low frequency ranges for copper intercalated n-HfS_2. The overall impedance and admittance response experimentally observed for copper intercalated n-HfS_2 in acetonitrile could be modelled by the equivalent circuits shown in Figure 3b. This circuit combines all the network elements explaining experimental observations in the high and low frequency regions. In these equivalent circuits the capacitance element C_o associated with reversible copper intercalation may be omitted in the high frequency region, whereas n-HfS_2 space charge capacitance C_{sc} may be eliminated at lower frequencies.

To investigate the influence of intercalated copper on n-HfS_2 C_{sc} in acetonitrile, impedance and admittance responses were analyzed as previously described by others[16,17]. C_{sc} for ||-c oriented n-HfS_2 in acetonitrile was obtained by subtracting susceptance values associated with cell resistance, R_{el}, from measured susceptance and by extrapolating capacitance data to infinite frequency (Figure 8). A value for C_{sc} of $\approx 3.2 \times 10^{-7}$ F/cm^2 at -0.295V vs. SCE was obtained, higher than 2.5×10^{-7} F/cm^2 at -0.103V vs. SCE determined in a previous study[18] by us using similar single crystal material, as expected at the more negative electrode potential used here. The dark C_{sc} for n-HfS_2 increased to 1.4×10^{-6} F/cm^2 after intercalating copper at -0.26V vs. SCE and remained essentially constant during the intervening (129 min.) intercalation (Figure 9). The potential of the dark n-HfS_2 electrode after 10-129 min. intercalation was relatively constant and remained at ≈-0.1V vs. SCE during 129 min. of intercalation. This suggested an equilibrium concentration of intercalated copper present after about 10 min. with further intercalation resulting in deeper copper incorporation into the crystal structure. For longer copper deposition times than 129 min. unit activity copper was evident on the n-HfS_2 surface after which the OCP became -0.4V vs. SCE. Cyclic

voltammograms for copper intercalated n-HfS_2 in acetonitrile are shown in Figure 10. The current peak corresponding to the reversible intercalation of copper was found to increase somewhat with time as the degree of copper intercalation was increased. Again this suggested that the semiconductor surface came relatively quickly to equilibrium (within ≅10 min.) in the concentration of intercalated copper. For single crystal n-HfS_2 used in this work the initial photopotential obtained prior to intercalation was 217mV under 100mW/cm^2 ELH illumination, but was found to decrease to 55mV upon initial copper intercalation, 36mV after 5 min. at ≅10μA and 18mV after 10 min. No photopotential was observed after 42 min.

To gain further insight into the influence of intercalated copper on the behavior of n-HfS_2 admittance spectroscopy analysis of the admittance data was performed[21,22]. Results of this analysis are summarized in Figure 11. In the simplest case the n-HfS_2/electrolyte interface was assumed to consist of the space charge capacitance, C_{sc}, connected in series with a bulk conductance G_{el}. By comparing real and imaginary parts of the admittance equation for such an equivalent circuit, with the appropriate in-phase admittance components being obtained experimentally, the following relationship can be obtained:

$$G/\omega = \frac{\omega\, C_{sc}^2\, G_{el}}{G_B^2 + (\omega C_{sc})^2} \qquad (6)$$

where G represents the measured in-phase cell conductance. By plotting G/ω vs. ω a maximum was given at

$$G/\omega_{max} = C_{sc}/2 \qquad (7)$$

from which the space charge capacitance was determined. The peak G/ω (where G corresponds to the total cell conductance) was identified with the n-HfS_2 space charge capacitance (curve A). Upon introducing CuCl into the electrolyte (curves B-D) evidence for an additional parameter in the equivalent circuit became evident. This was interpreted as corresponding to a Faradaic conductance in parallel to C_{sc} as shown by a linear log G/ω vs. log ω relationship[21,22]. At sufficiently low frequencies the measured conductance became equal to the Faradaic conductance. Thus, increased conductance in the low/middle frequency region for copper intercalated HfS_2 gave evidence for the Faradaic intercalation-deintercalation reaction of copper. Unfortunately, increased conductance by the cell due to electron transfer at the interface

overshadows effects from the space charge capacitance. Deposition of copper onto the n-HfS_2 surface (curve E) shifted the conductance associated with the Faradaic reaction to even higher values. This suggested a higher exchange current density for this copper compared to that intercalated within the n-HfS_2.

It has been suggested that metals intercalated into group IVB TMDs result in the formation of energy levels within the band gap[7]. Copper deintercalation from voltammetric experiments occur even in the absence of any measurable photopotential suggesting the formation of energy levels close to the conduction band during intercalation. A similar explanation has been postulated[23] for cyclopropylamine intercalated $HfSe_2$. Intercalation by copper or iron into ZrS_2 and HfS_2 by others[13] has indicated that the electrode remains semiconducting at intercalation levels below $HfCu_{0.22}S_2$. It is probable that in work discussed here the degree of copper intercalation may have been higher than calculated using the diffusion coefficient $10^{-8}cm^2/sec$. To preserve n-HfS_2 semiconducting properties the total charge passed during copper intercalation should be lower than 0.3C per $1cm^2$ for ||-c oriented material. Such intercalating photoelectrodes may eventually be of interest in liquid non-aqueous or solid polymer electrolyte cells. In the latter cells the deintercalated transition metal ions would be stored in close proximity to the electrode/solid electrolyte interfacial region.

CONCLUSION

The ||-c oriented n-HfS_2/non-aqueous electrolyte interface can be modelled by equivalent circuits consisting of space charge capacitance, cell resistance and frequency dependent R-C elements. In the presence of intercalated copper in n-HfS_2 increased Faradaic conduction became evident related to intercalation-deintercalation at the interfacial region. The space charge capacitance of n-HfS_2 in acetonitrile was obtained by eliminating the capacitive response of frequency dependent elements and was found to be of the order 10^{-7} F/cm^2. This increased to 10^{-6} F/cm^2 after intercalating > 18m/o copper into this semiconductor. Electrochemical copper deintercalation proceeded in the dark suggesting that the semiconductor became degenerate at this degree of intercalation with a high population of electrons being localized close to the n-HfS_2 conduction band.

ACKNOWLEDGEMENT

This work was supported in part by the Office of Naval Research.

REFERENCES

1. J. A. Wilson and A. D. Yoffee, Adv. Phys., 18, 193 (1969).
2. E. Mooser, Ed., Physics and Chemistry of Materials with Layered Structures, Reidel, Dordrecht, Boston, MA, 1976.
3. R. B. Murray, R. A. Bromley and A. D. Yoffee, J. Phys. C. Solid State Phys., 5, 746 (1972).
4. L. F. Mattheiss, Phys. Rev., B8, 3719 (1973).
5. H. Tributsch, J. Electrochem. Soc., 128, 1261 (1981).
6. H. Tributsch, Faraday Discuss. Chem. Soc., 70, 190 (1981).
7. M. Abramovich, H. Tributsch and O. Gorochov, J. Electroanal. Chem., 153, 115 (1983).
8. M. Abramovich and H. Tributsch, J. Electroanal. Chem., 138, 121 (1982).
9. H. Tributsch, Appl. Phys., 23, 61 (1980).
10. F. R. Gamble and T. H. Geballe, Treatise on Solid State Chemistry, Vol 3, Plenum Press, New York, 1976.
11. G. V. Subbor Rao and J. C. Tsang, Mater. Res. Bull., 9, 921 (1974).
12. M. S. Whittingham, U.S. Patent 4,040,917 (1977).
13. B. G. Yacobi, F. W. Boswell and J. M. Corbett, J. Phys. C. Solid State Phys., 12, 2189 (1979).
14. W. Kantele, H. Gerischer and H. Tributsch, Ber. Bunsenges Phys. Chem., 83, 1000 (1979).
15. H. Tributsch, Structure and Bonding, 49, 128 (1982).
16. J. F. McCann, S. P. S. Badwal and J. Pezy, J. Electroanal. Chem., 118, 115 (1981).
17. J. F. McCann and S. P. S. Badwal, J. Electrochem. Soc., 129, 551 (1982).
18. K. W. Semkow, N. U. Pujare and A. F. Sammells, J. Electrochem. Soc., (submitted).
19. S. P. S. Badwal and H. J. de Bruin, Phys. Status Solidi A, 54, 261 (1979).
20. I. D. Raistrick, C. Ho and R. A. Huggins, J. Electrochem. Soc., 123, 1469 (1976).
21. P. A. Smith, "Electrical Characterization of Polycrystalline and Photoelectrochemical Solar Cells", M. S. Thesis, Colorado State University, Ft. Collins, CO (1980).
22. J. Dubow and R. Krishnar, "Novel Concepts in Electrochemical Solar Cells", SERI Final Report, Contract No. XS-0-9272-1 (October 1981).
23. A. R. Beal and W. Y. Liang, Phil. Mag., 27, 1397 (1973).

FIGURE CAPTIONS

Figure 1. Impedance response for ||-c oriented n-HfS_2 in CH_3CN (0.1M $TBAPF_6$) at OCP (-0.295V).

Figure 2. Admittance response for ||-c oriented n-HfS_2 in CH_3CN (0.1M $TBAPF_6$) at OCP (-0.295V).

Figure 3a. Equivalent circuits for ||-c oriented n-HfS_2 in CH_3CN (0.1M $TBAPF_6$) at high (A) and low (B) frequencies.

Figure 3b. Equivalent circuit for copper intercalated ||-c oriented n-HfS_2 in CH_3CN (0.1M $TBAPF_6$ + 0.001M CuCl) at high (A) and low (B) frequencies.

Figure 4. Impedance response for ||-c oriented n-HfS_2 in CH_3CN (0.1M $TBAPF_6$ + 0.001M CuCl) after 42 minutes copper intercalation (≅10μA) at -0.26V vs. SCE.

Figure 5. Admittance response for ||-c oriented n-HfS_2 in CH_3CN (0.1M $TBAPF_6$ + 0.001M CuCl) after 42 minutes copper intercalation (≅10μA) at -0.26V vs. SCE.

Figure 6. Impedance response for ||-c oriented n-HfS_2 in CH_3CN (0.1M $TBAPF_6$ + 0.001M CuCl) after 129 minutes copper intercalation (≅10μA) at -0.26V vs. SCE.

Figure 7. Admittance response for ||-c oriented n-HfS_2 in CH_3CN (0.1M $TBAPF_6$ + 0.001M CuCl) after 129 minutes copper intercalation (≅10μA) at -0.26V vs. SCE.

Figure 8. Frequency dependent capacitance for ||-c oriented n-HfS_2 in CH_3CN (0.1M $TBAPF_6$) at OCP (-0.295 vs. SCE). Geometric electrode area 0.06cm^2.

Figure 9. Frequency dependent capacitance for ||-c oriented n-HfS_2 in CH_3CN (0.1M $TBAPF_6$ + 0.001M CuCl) after copper intercalation at -0.26V vs. SCE (≅10μA) for 10 minutes (curve A), 42 minutes (curve B) and 129 minutes (curve C). Geometric electrode area 0.06cm^2.

Figure 10. Cyclic voltammograms for ||-c oriented n-HfS_2 in CH_3CN (0.1M $TBAPF_6$ + 0.001M CuCl) after copper intercalation of -0.26V (≅10μA) for A) 2 min., B) 5 min., and C) 10 min. Scan rate: 20mV/sec.

Figure 11. Relationship between G/ω and ω for ||-c oriented n-HfS_2 in CH_3CN (0.1M $TBAPF_6$) without (curve A) and with (curves B-E) 0.001M CuCl. Curve A at OCP -0.295V vs. SCE. Curves B, C and D after 10, 42 and 129 minutes respectively copper intercalation at -0.26V (≅10μA) (OCP -0.1V); E after 130 minutes when copper deposition on the n-HfS_2 surface became evident (OCP -0.4V vs. SCE).

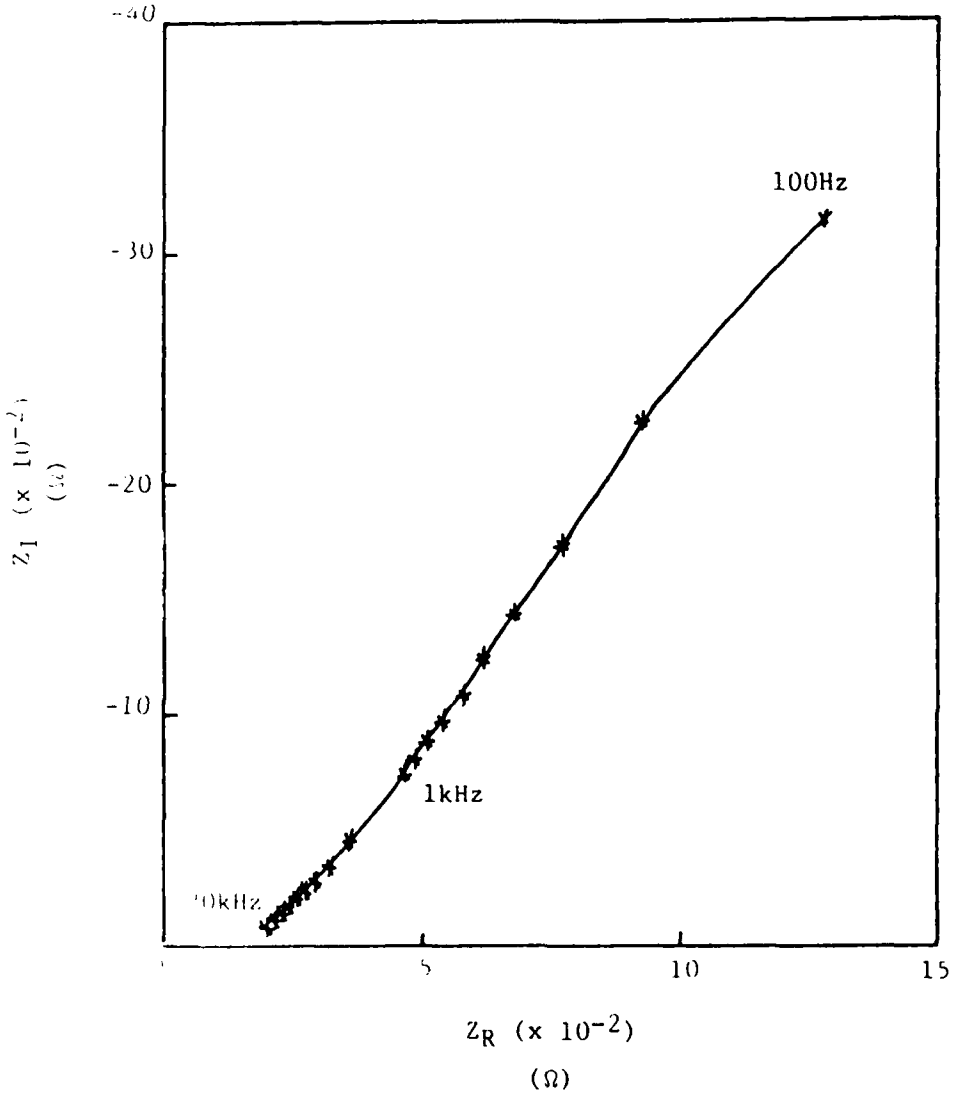

Figure 1 Impedance response for ∥-c oriented n-HfS_2 in CH_3CN (0.1M $TBAPF_6$) at OCP (-0.295V).

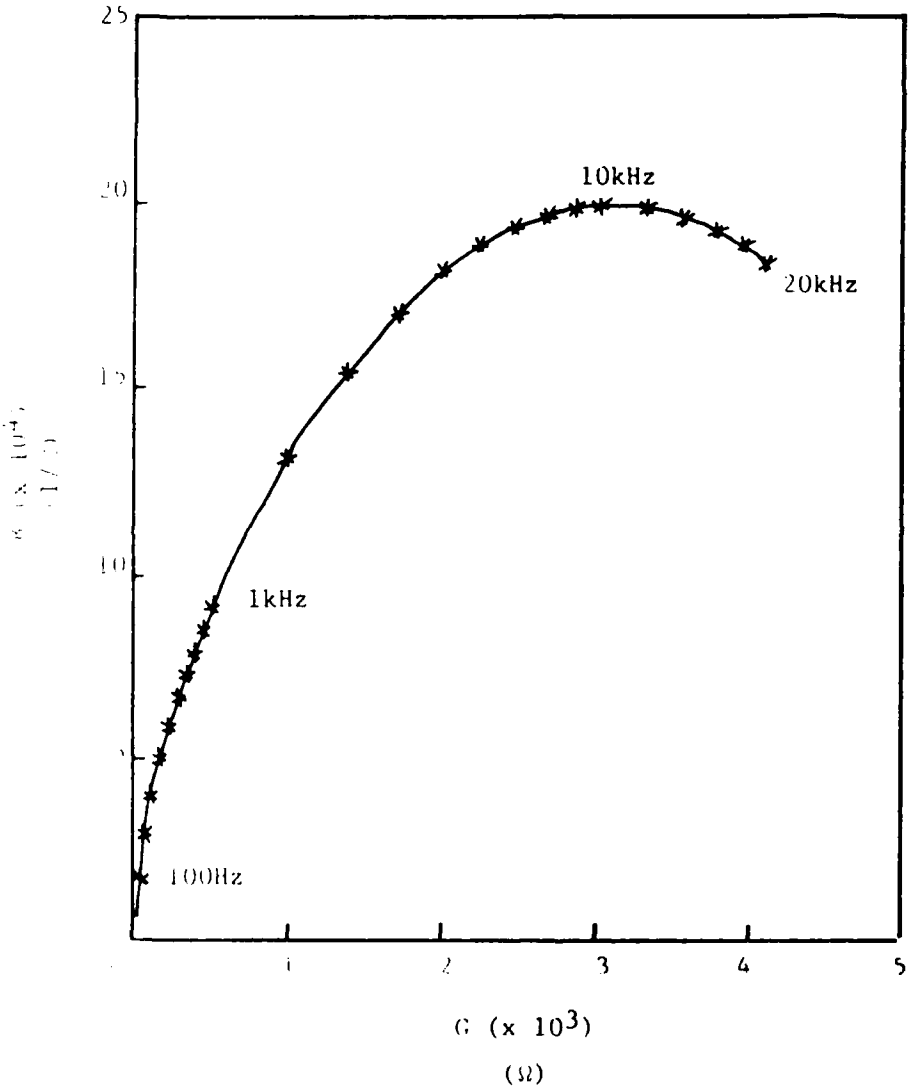

Figure 2. Admittance response for ll-c oriented n-HfS_2 in CH_3CN (0.1M $TBAPF_6$) at OCP (-0.295V).

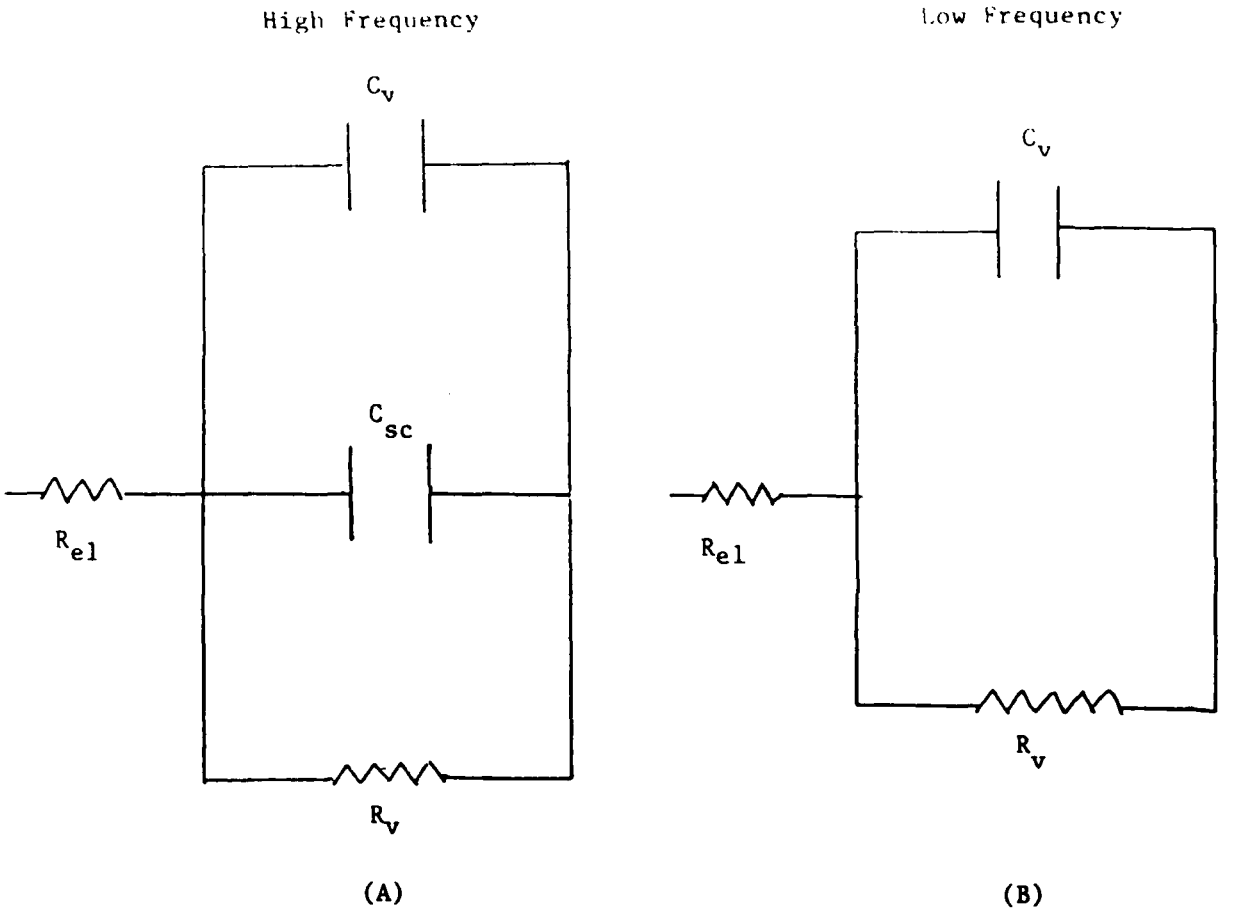

Figure 3a. Equivalent circuits for ⊥-c oriented n-HfS_2 in CH_3CN (0.1M $TBAPF_6$) at high (A) and low (B) frequencies.

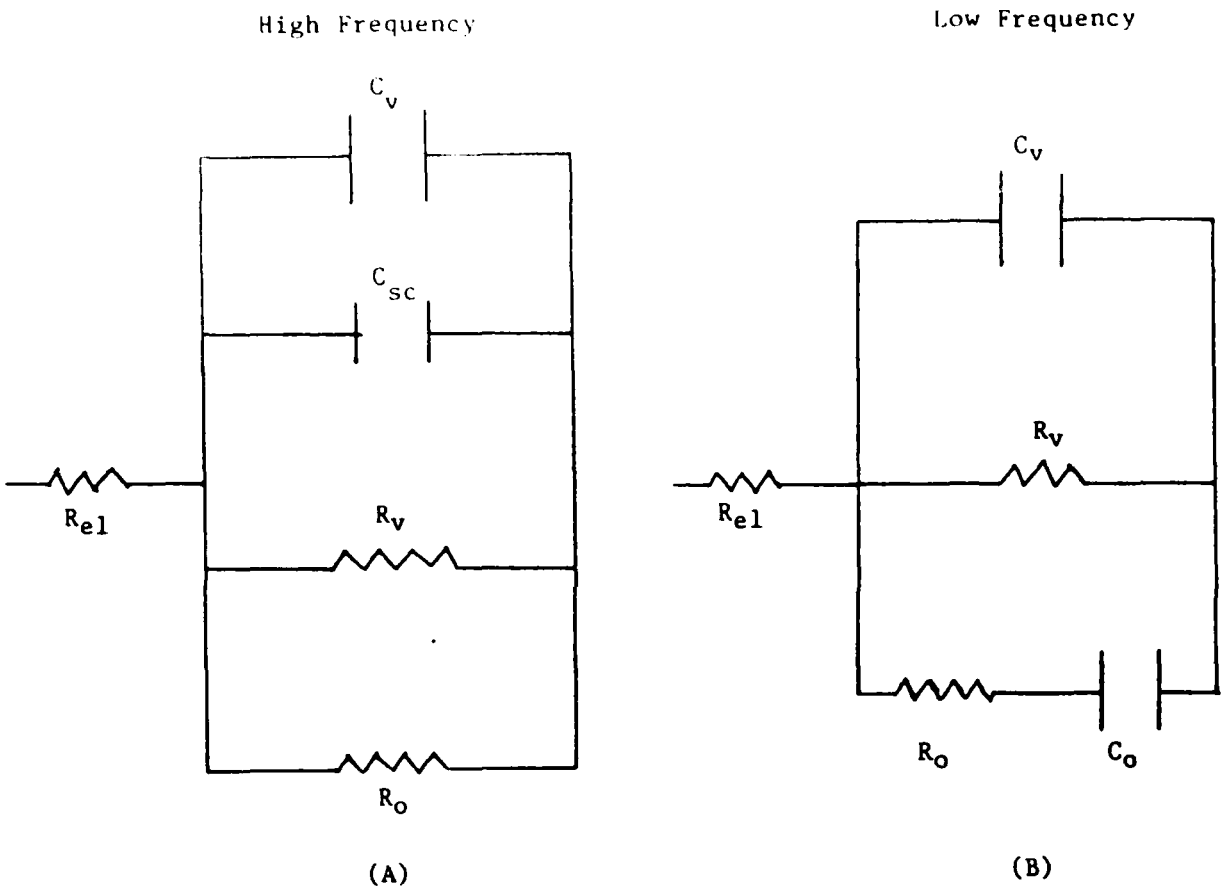

Figure 3b. Equivalent circuit for copper intercalated ⊥-c oriented n-HfS_2 in CH_3CN (0.1M $TBAPF_6$ + 0.001M CuCl) at high (A) and low (B) frequencies.

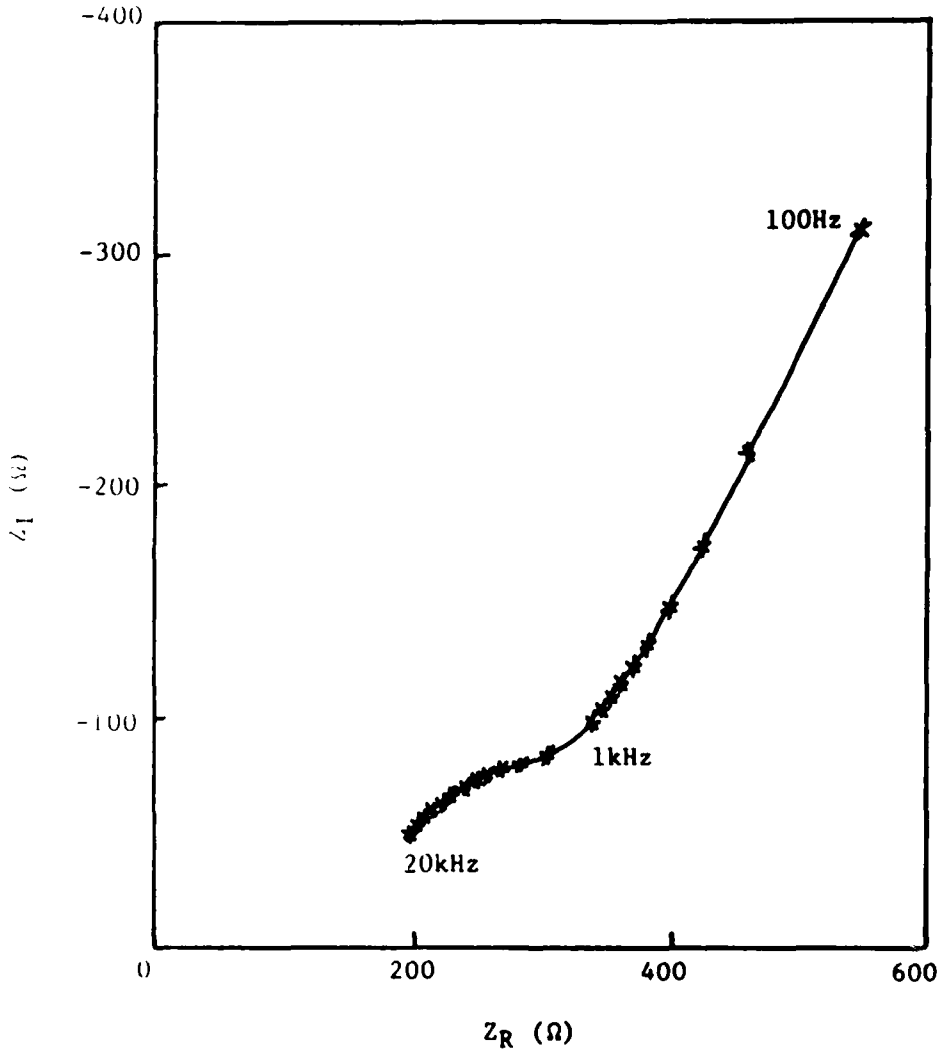

Figure 4. Impedance response for ⊥-c oriented n-HfS_2 in CH_3CN (0.1M $TBAPF_6$ + 0.001M CuCl) after 42 minutes copper intercalation (≈10μA) at -0.26V vs. SCE.

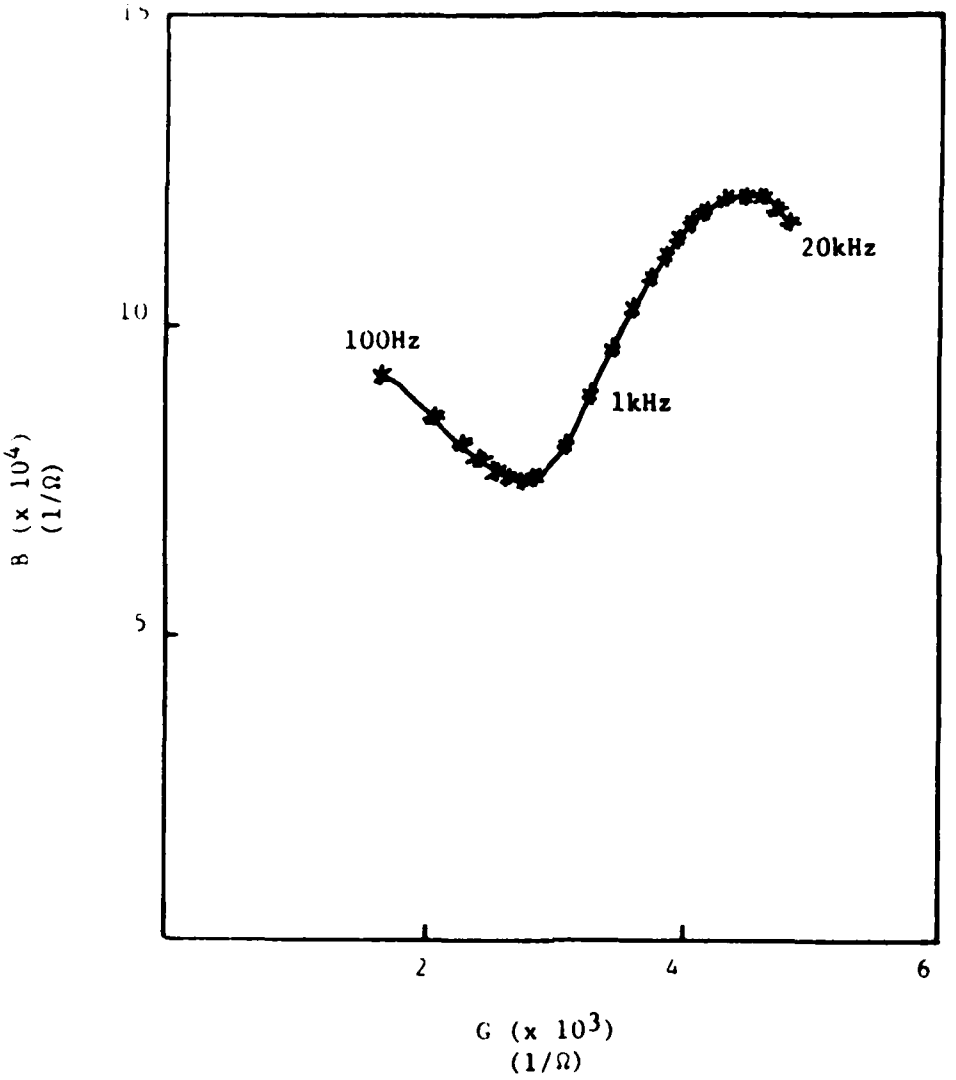

Figure 9. Admittance response for ⊥-c oriented n-HfS_2 in CH_3CN (0.1M $TBAPF_6$ + 0.001M CuCl) after 42 minutes copper intercalation (≈10uA) at -0.26V vs. SCE.

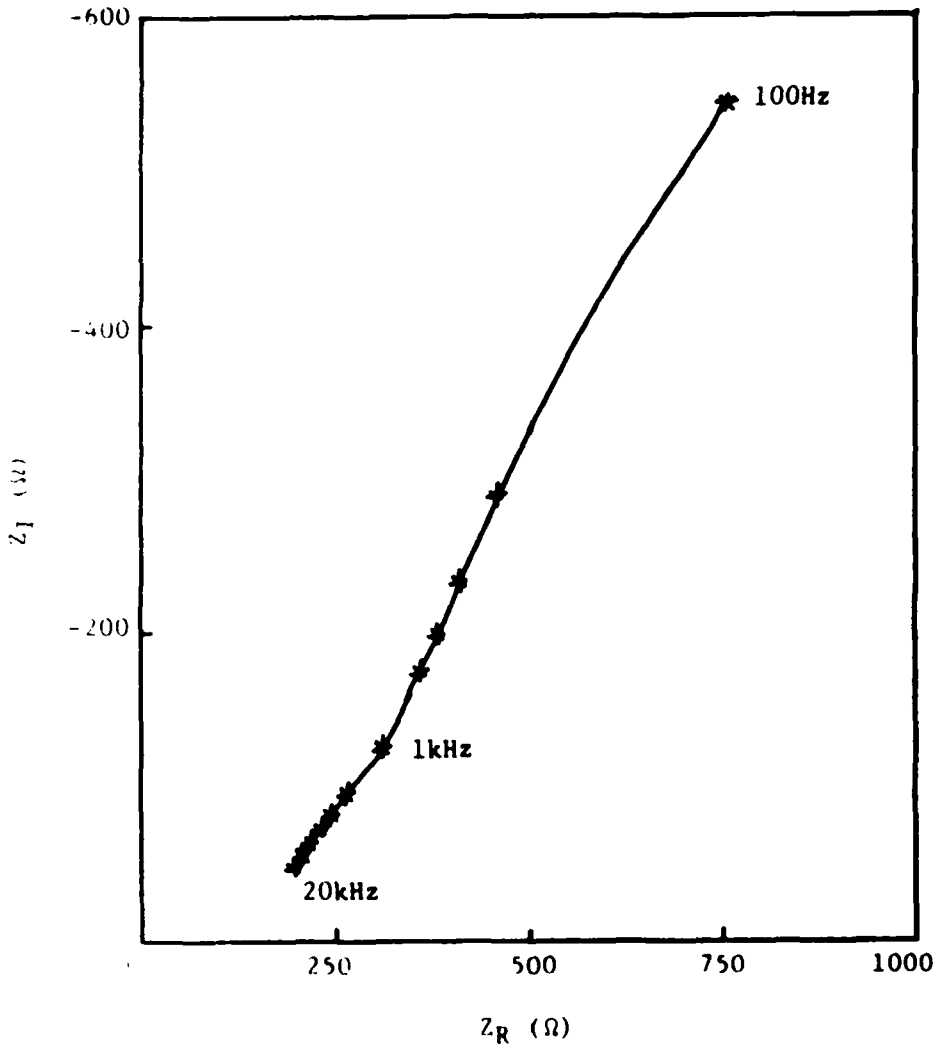

Impedance response for ⊥-c oriented n-HfS_2 in CH_3CN + .1M $TBAPF_6$ + 0.001M CuCl) after 129 minutes copper intercalation (≈10uA) at -0.26V vs. SCE.

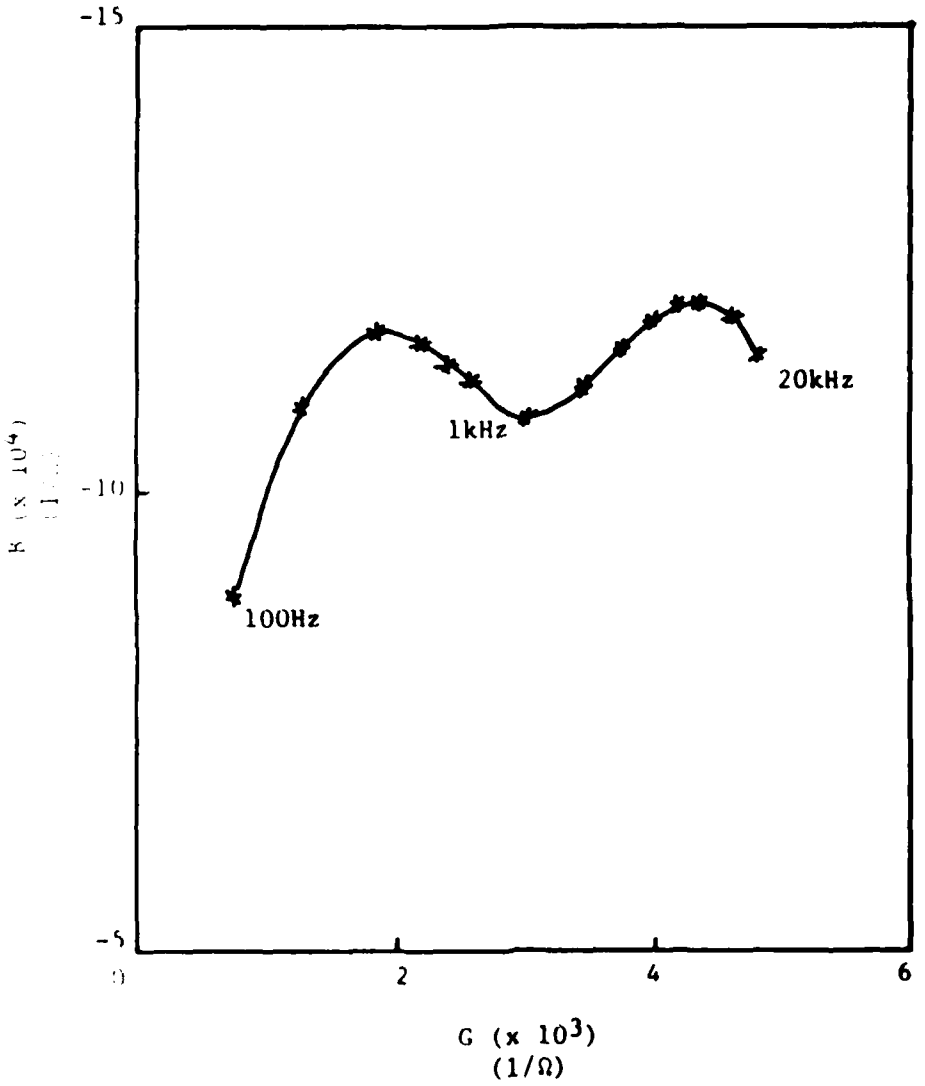

Figure 7. Admittance response for n-c oriented n-HfS_2 in CH_3CN (0.1M $TBAPF_6$ + 0.001M CuCl) after 129 minutes copper intercalation (≅10μA) at -0.26V vs. SCE.

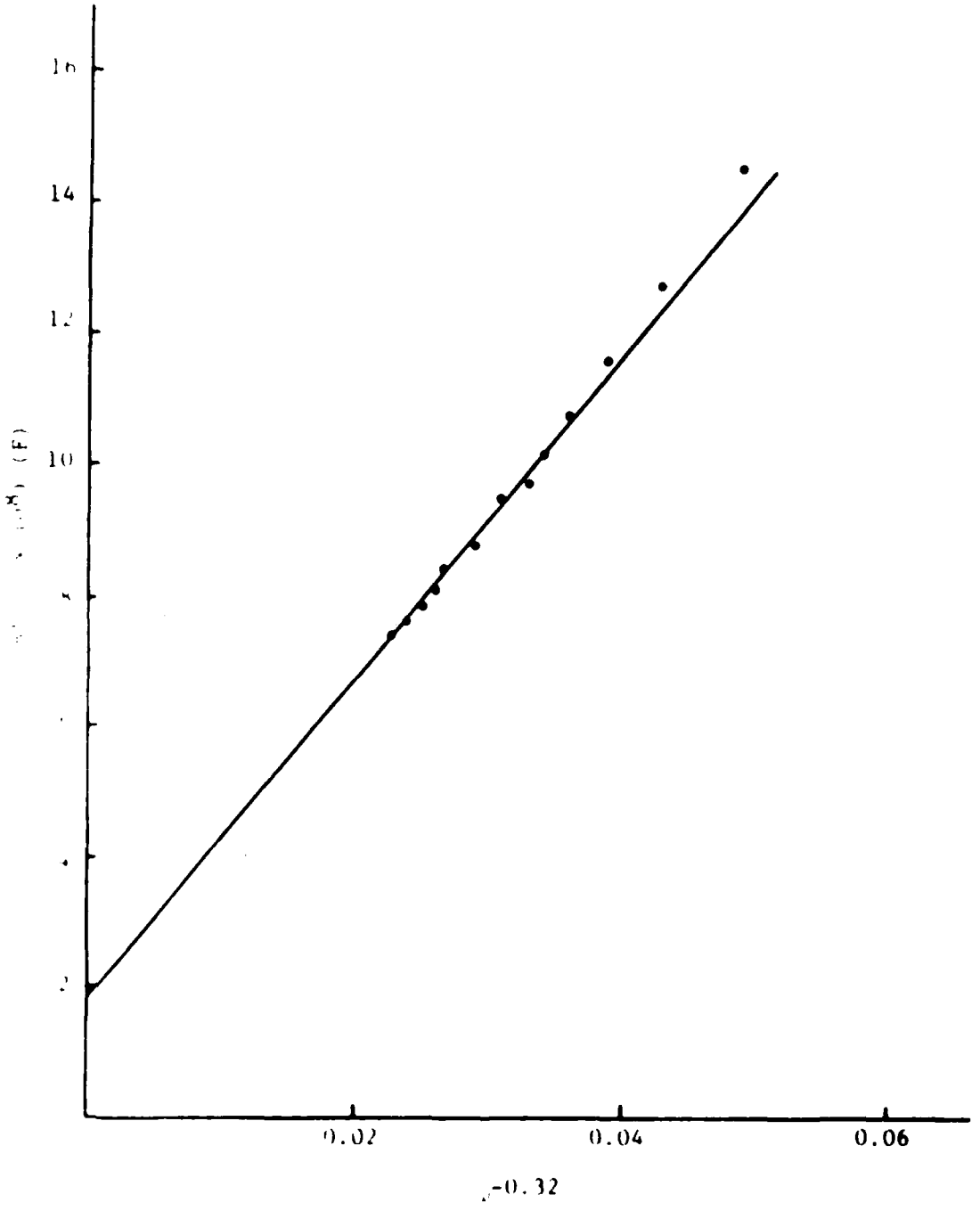

dependent capacitance for ⊥-c oriented n-HfS_2 in CH_3CN
NEt_4 at OCP = -0.295 vs. SCE). eometric electrode area

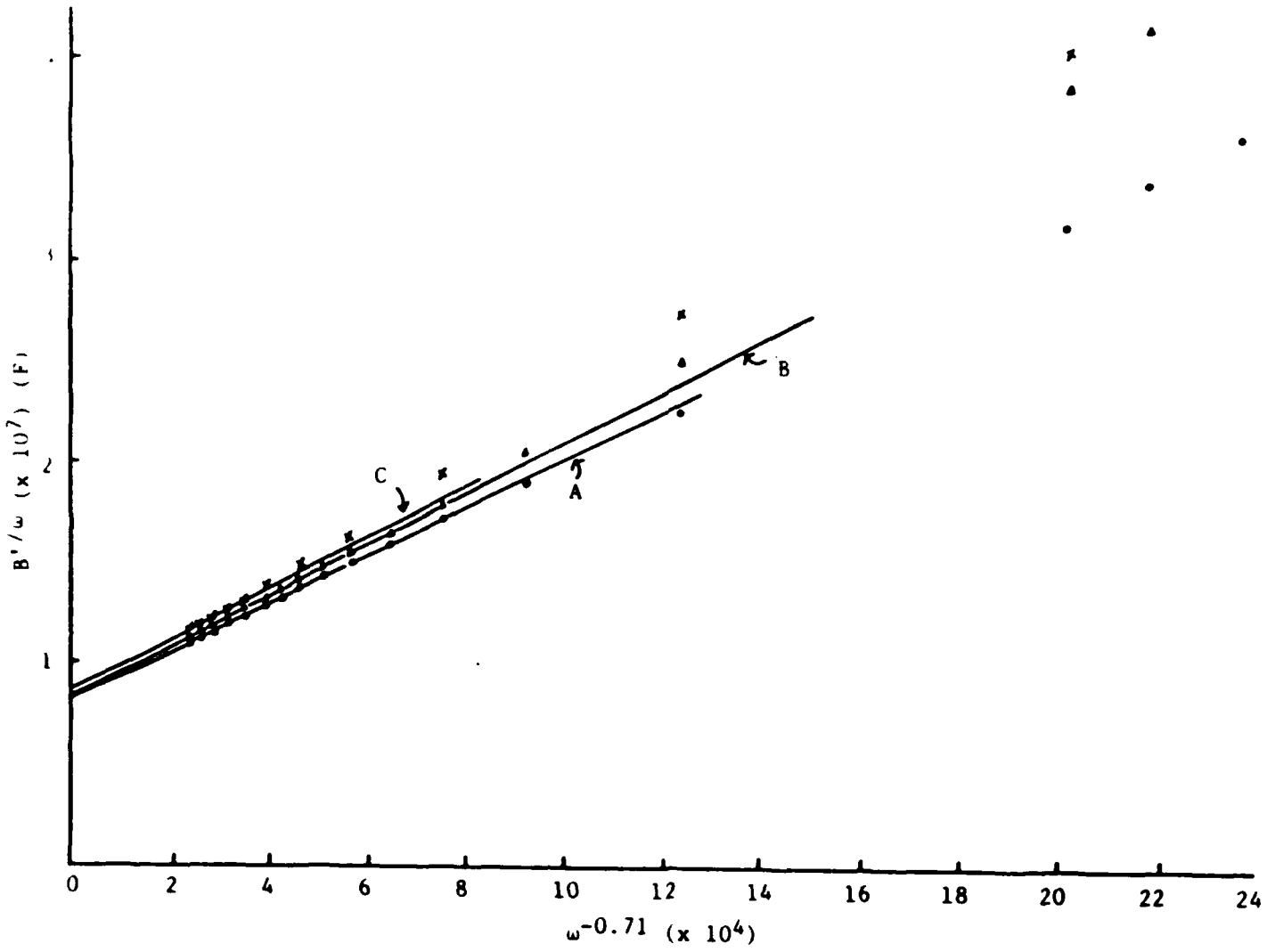

Figure 9. Frequency dependent capacitance for ⊥-c oriented n-HfS_2 in CH_3CN (0.1M $TBAPF_6$ + 0.001M CuCl) after copper intercalation at -0.26V vs. SCE (≈10μA) for 10 minutes (curve A), 42 minutes (curve B) and 129 minutes (curve C). Geometric electrode area 0.06cm^2.

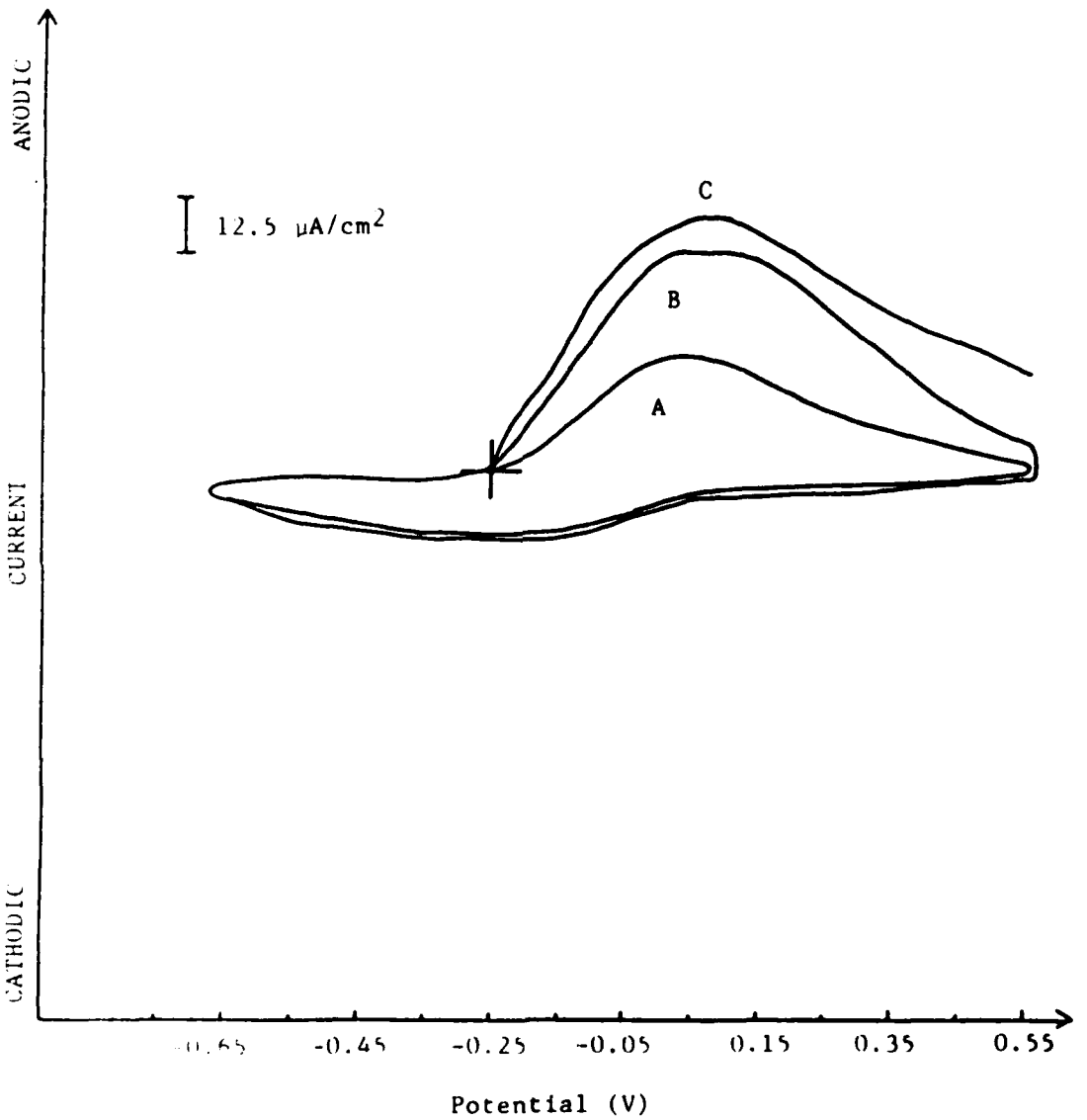

Figure 10. Cyclic voltammograms for ||-c oriented n-HfS_2 in CH_3CN (0.1M $TBAPF_6$ + 0.001M CuCl) after copper intercalation of -0.26V (≅10μA) for A) 2 min., B) 5 min., and C) 10 min. Scan rate: 20mV/sec.

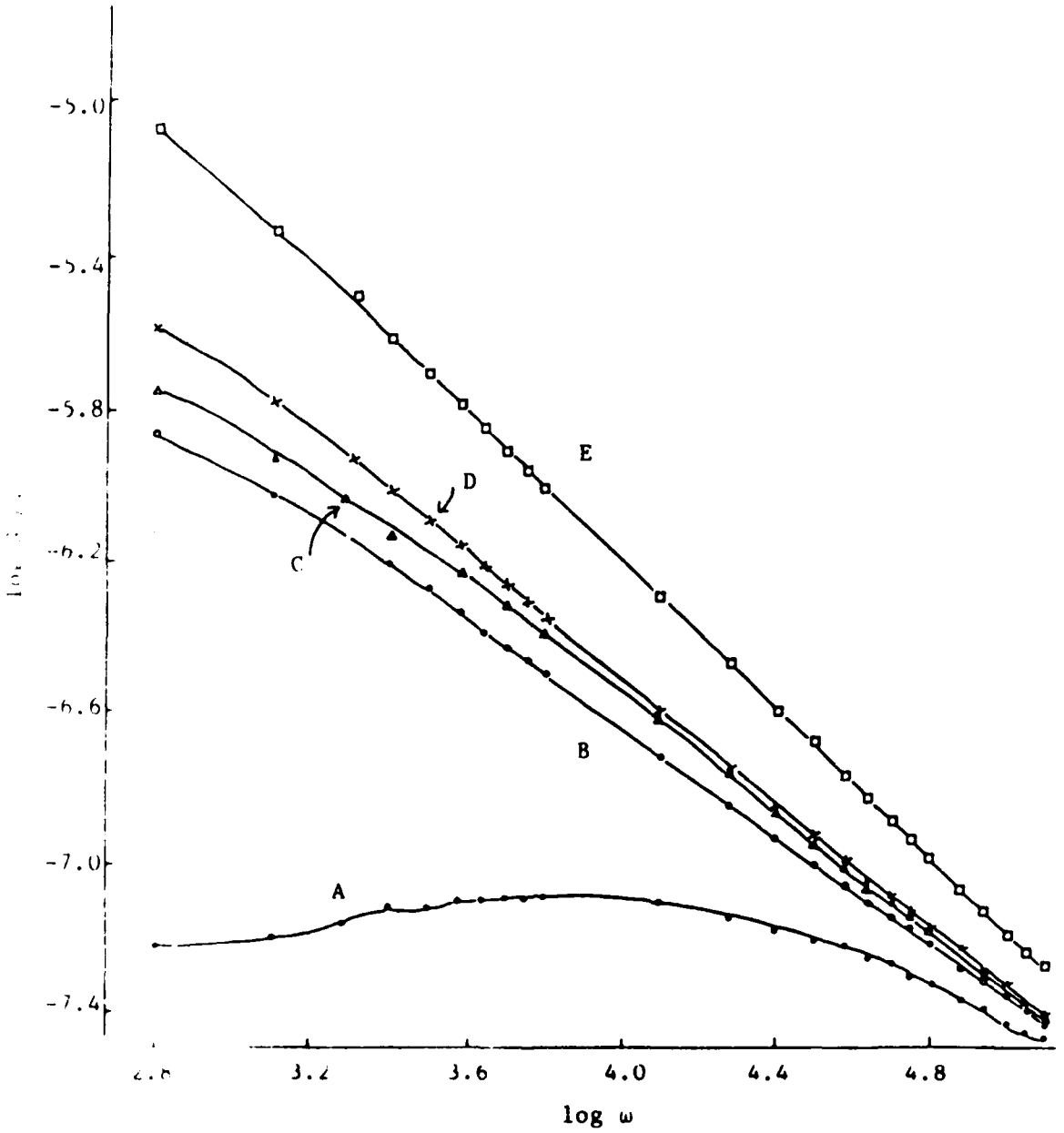

Figure 11. Relationship between G/ω and ω for II-c oriented n-HfS_2 in CH_3CN (0.1M $TBAPF_6$) without (curve A) and with (curves B-E) 0.001M CuCl. Curve A at OCP -0.295V vs. SCE. Curves B, C and D after 10, 42 and 129 minutes respectively copper intercalation at -0.26V (≈10μA) (OCP -0.1V); E after 130 minutes when copper deposition on the n-HfS_2 surface became evident (OCP -0.4V vs. SCE).

END

9-87

DTIC